

Preparation of Porous Honeycomb Monolith from UV-Curable Monomer/Dioxane Solution via Unidirectional Freezing and UV Irradiation

Rika Okaji, Kentaro Taki, Shinsuke Nagamine, Masahiro Ohshima

Department of Chemical Engineering, Kyoto University, Kyoto 615-8510, Japan

Received 28 February 2011; accepted 4 November 2011

DOI 10.1002/app.36443

Published online 31 January 2012 in Wiley Online Library (wileyonlinelibrary.com).

ABSTRACT: A well-ordered micrometer-scale honeycomb monolith porous polymeric material with aligned channels was successfully prepared from UV-curable urethane diacrylate monomer and 1,4-dioxane solutions by conducting unidirectional freezing, photopolymerization, and sublimation of the frozen solvent. UV light was irradiated into the frozen solution, and the monomer was photopolymerized and solidified in a template of 1,4-dioxane crystals. The effects of monomer concentration, freezing rate, and viscosity of the solution on the porous structure were investigated. High monomer concentration increases the solution viscosity, decreases the diffusivity of solute, and consequently, increases the degree of the

supercooling. Thus, the pore size was decreased, and the channel wall feature was changed from smooth to dendrite as the solution viscosity increased. Pre-UV irradiation was also conducted before the unidirectional freezing process so as to control the solution viscosity and change the porous structure. Experiments elucidated that the solution viscosity is one of the key factors of determining the cell structure in the unidirectional freezing technique. © 2012 Wiley Periodicals, Inc. *J Appl Polym Sci* 125: 2874–2881, 2012

Key words: freezing; porous material; microstructure; polymerization; polymer processing; morphology

INTRODUCTION

Unidirectional freeze/freeze-drying is an easy and cost-effective method for preparing porous polymeric materials: a solution mixture of polymers and solvents is frozen in one direction, the regularly aligned solvent crystal grows in the freezing direction, the solute material is solidified and structured using the crystalline structure as a template, and then, the crystal is allowed to sublimate by drying *in vacuo* and the aligned channel structure can be prepared. The method can be applied not only to polymer solution^{1–5} but sol/gel,^{6–9} hydrogels,¹⁰ ceramic slurry,^{8,11–17} and inorganic particles colloidal solutions.^{9,18,19} Interest in the method is dramatically increasing^{2,3,19–23} because of its inherently high controllability of its porous and fiber structure.

The porous structures absolutely depend on the solvent crystal morphology. There have been several studies for investigating the factors of affecting the crystal morphology and the resulting porous structure. Material concentration,^{1,12} particle size of ceramic slurry,²⁴ addition of impurity component,^{2,3} and freezing rate^{11,25–27} have been investigated as the

key factors. The Mullins-Sekerka instability theory²⁸ and the Jackson and Hunt's solidification theory of metallic eutectic alloy²⁹ were used to relate the key factors with the solute porous structure qualitatively.

As far as the authors concerned, no article had discussed in past the effect of solution viscosity in unidirectional freezing process on the porous structure. Thus, in this study, the viscosity of the solution was investigated as another key factor of affecting the porous structure in unidirectional freezing of polymer/solvent solutions. Here, *in situ* crosslinking was integrated into the unidirectional freezing methods. UV-curable monomer was used as a crosslinking monomer, which could be initiated by UV-light irradiation. Pre-UV irradiation was conducted before the unidirectional freezing process so as to control the solution viscosity while keeping the solute weight concentration in solution. The effects of the solution viscosity on the pore size and structure were examined by changing the UV-irradiation time.

In the previous works, the controllability of the wall thickness¹¹ and the microscale channel diameter² had been mainly discussed. It has been pointed out in the discussions that the average diameter of microchannel increased with the decrease in freezing rate^{11,23,30} as well as in solute material concentration,^{2,12} and that the average wall thickness increased either with the decrease in freezing rate or the increase in solute material concentration. The

Correspondence to: R. Okaji (okaji@cheme.kyoto-u.ac.jp).

decrease in solute concentration lowers the degree of constitutional supercooling, reduces the solvent crystal growth rate and increases channel diameter. Thus, to prepare large cells from this polymer/solvent system by the unidirectional freezing method, it is necessary to increase the diffusivity of the solute in the solution. Low molecular weight polymer was used for that purpose. However, in general, a lower molecular weight polymer does not have enough toughness to uphold the shape of the desired product. From this aspect, the UV-curable monomer provides an advantage for use in the unidirectional freezing process, which has a low molecular weight during the freezing process and then is transformed to having a higher molecular weight by photopolymerization, thus keeping its shape after freeze drying.

MATERIALS AND METHODS

Materials

The UV-curable monomer of urethane diacrylate (M1100) was supplied by Toagosei, Japan. 1,4-Dioxane, dehydrated as solvent, and diphenyl(2,4,6-methylbenzoyl)phosphine oxide (TPO, Wako) as photoinitiator were purchased from Wako Pure Chemicals, Japan. Preliminary measurement of the average molecular weight of UV-curable monomer was conducted using gel permeation chromatography [polystyrene (PS) standard, chloroform eluent] and resulted in 20,000. For the reference, poly(L-lactic acid) (PLLA, $\overline{M}_W = 2.8 \times 10^5$, $\overline{M}_w/\overline{M}_n = 2.24$, density = 1.12) was used.² The average molecular weight, \overline{M}_W , the number average molecular weight, \overline{M}_n , and polydispersity, $\overline{M}_w/\overline{M}_n$ of the PLLA were measured by gel permeation chromatography (Shimadzu, model SPD-20A). The retention time and molecular weight were calibrated using PS standards.

Preparation of the solution

The UV-curable monomer M1100 was dissolved in 1,4-dioxane dehydrated at the predetermined concentrations of 3, 5, and 10 wt %. TPO was added to the solution at 1 wt % of the monomer. The solution was then stirred at 50°C for 1 h.

PLLA/dehydrated 1,4-dioxane single phase solution² was also prepared by dissolving PLLA into dehydrated 1,4-dioxane at 50°C. The concentration of PLLA in solution was changed at two levels, 3 and 5 wt %.

The kinetic viscosity of these solutions was measured with an Ubbelohde viscometer at 25°C. The density of the solutions was measured by weighing the specified volume of the solution. The solution viscosity was then calculated by multiplying the density and kinetic viscosity.

Unidirectional freezing and photopolymerization

The solution was poured into a polypropylene (PP) test tube of 1.2-mm wall thickness, 100 mm length, and 10-mm inner diameter, and immersed into a liquid N₂ bath at one of three different constant rates: 1.5, 3.5, or 7.5 cm/h. The solvent was frozen unidirectionally from the bottom of the tube upward. The PP tube was sealed with a cap before immersion. After the test tube was immersed and the solution was frozen completely, the solidified UV-monomer and dioxane sample was put into a temperature-controlled isothermal bath at -25°C for 1 h to raise the sample temperature. The desired temperature was that at which photopolymerization of UV-curable monomer could be initiated while keeping the solvent frozen. Then the test tube was removed from the isothermal bath and exposed to UV light for 3.0 min to polymerize the UV-curable monomer. The UV light was guided by a bundle of quartz fibers with collimator lens from a Mercury Xenon lamp light source (MUV-202-U, 200W, MORITEX). The incident light intensity was monitored using a UV radiometer (UT-150, USHIO, Japan) in which the maximum intensity wavelength was 365 nm. The UV intensity was set to 35 mW/cm². After curing the monomer of the microstructure by UV irradiation, the sample was dried *in vacuo* for 2 days.

Morphology characterization

The obtained microstructures were observed by scanning electron microscopy (SEM, upgraded Tiny-SEM 1540, Technex Lab, Japan). For SEM analysis, the dried samples were frozen by liquid nitrogen to prevent deformation while cutting with a razor blade in either a parallel or perpendicular direction to the freezing direction. The prepared samples were then coated with gold *in vacuo* before observation.

Freezing-point measurement

To measure the freezing-point depression of the sample solution as a function of UV-curable monomer concentration, the freezing-point measurement was conducted by adopting a simple laser transmittance scheme. The solution temperature was decreased at a rate of 0.7°C/min from a starting temperature of 20°C. The detailed scheme is found in the previous work.³

RESULTS AND DISCUSSION

Honeycomb structure

A honeycomb porous structure was successfully produced from a 3-wt % UV-curable monomer solution by unidirectional freezing at a tube immersion rate

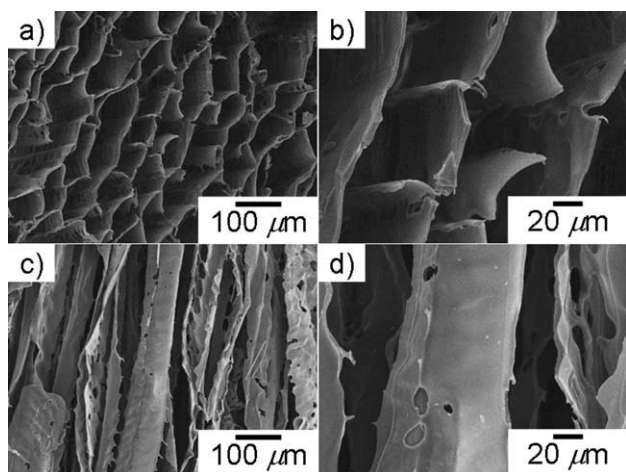


Figure 1 SEM micrographs of the honeycomb monolith structure of the cross section perpendicular to the freezing direction (a and b), and the cross section parallel to the freezing direction (c and d). (b) and (d) are the magnified views of (a) and (c), respectively.

of 1.5 cm/h. Figure 1 shows micrographs of the cross-sectional area parallel to the freezing direction [Fig. 1(c,d)], and the cross-sectional area perpendicular to the freezing direction [Fig. 1(a,b)]. Clearly, the honeycomb and channel (microtube) structures were formed in the cross-sectional area perpendicular and parallel to the freezing direction, respectively. The average diameter of the microtube was 80 μm . Compared to the pore size of the honeycomb monolith made from poly(L-lactide)/1,4-dioxane solution,² which was about 20 μm in diameter, the use of UV-curable monomer increased pore diameter in the honeycomb structure.

Effect of freezing rate on cell structure

To investigate the effect of freezing rate on the porous structures, 1,4-dioxane solution with 3 wt % monomer was frozen at three different rates, 1.5, 3.5, and 7.5 cm/h. Figure 2 indicates SEM micrographs of the resulting porous materials. The average channel diameter was measured from the micrograph, and the results are presented in Figure 3. Figure 3 also shows a trend in which increasing the freezing rate reduces the channel diameter. The results agreed with the previous studies on the unidirectional freezing of the polymer solution^{2,3}: the faster the freezing rate, the shorter the wavelength of solvent crystals and the smaller the channel diameters. As indicated in Figure 2(c,f), when the freezing rate exceeded 7.5 cm/h, the interface between the solvent crystals and solution became unstable. This phenomenon causes a dendritic structure to form on the channel wall, and smaller pores interconnecting the channels eventually formed on the wall.

Effect of UV-curable monomer concentration on cell structure

To investigate the effect of monomer concentration on porous structure, the solutions were frozen at a constant freezing rate of 3.5 cm/h by testing the monomer concentration in the solutions at three different levels: 3, 5, and 10 wt %. Figure 4 shows the SEM micrographs of the porous materials prepared from the solutions with these three monomer concentrations. The micrographs show that the smooth channel wall structure was transformed to dendrite structure by increasing the monomer concentration. The walls were smooth at 3 wt % [Fig. 4(a,d)], and

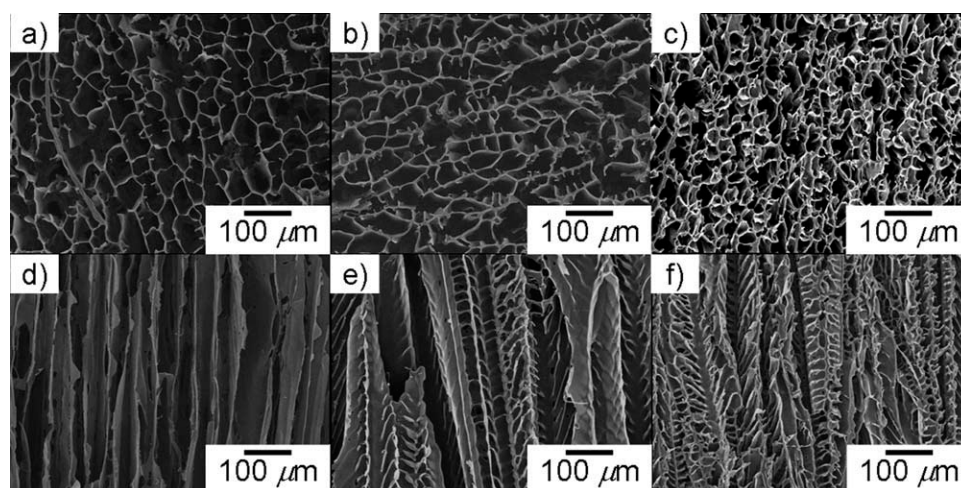


Figure 2 Effect of freezing rate on honeycomb structure. SEM micrographs of porous materials prepared from 3 wt % monomer/1,4-dioxane solution: (a–c) cross section perpendicular to the freezing direction and (d–f) cross section parallel to the freezing direction. Immersion rates into the liquid nitrogen bath were (a and d) 1.5 cm/h, (b and e) 3.5 cm/h, and (c and f) 7.5 cm/h.

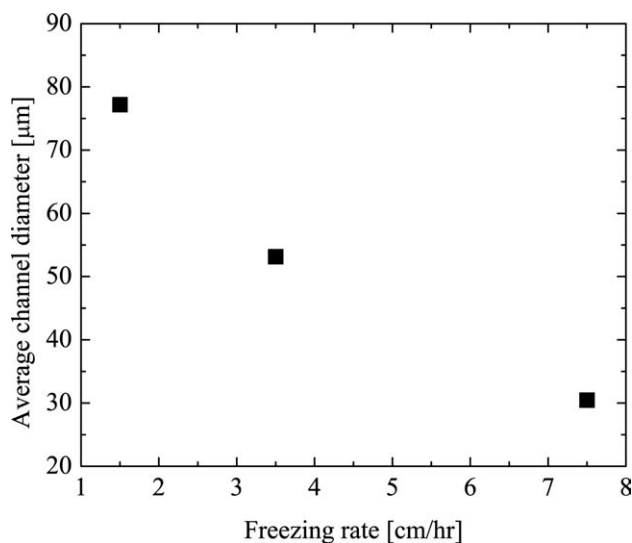


Figure 3 Average channel diameter of microchannels perpendicular to the freezing direction versus freezing rate at a monomer concentration of 3 wt %.

fishbone-like structures appeared at 5 wt % [Fig. 4(b,e)] and 10 wt % [Fig. 4(c,f)].

The transformation from a smooth to dendrite structure could be explained by the increase in the degree of supercooling. When freezing the solute-solvent system, the freezing temperature of the solvent is reduced by the solute. In our system, the UV-curable monomer dissolved in the solution could induce the freezing-point depression. The reduction of freezing temperature increases the degree of the supercooling thus increasing the instability of the solvent crystal growth. As a result, the porous structure tends to be more dendritic as the solution concentration increases.²⁸

Solute-induced freezing-point depression

Figure 5 shows the freezing-point and solute concentration curves of UV-curable monomer/1,4-dioxane solutions. The freezing point of dehydrated 1,4-dioxane alone is 12.0°C. For the UV-curable monomer/1,4-dioxane system, it decreases to 1°C as the monomer concentration increases to 10 wt %. The degree of freezing-point reduction is determined by the colligative properties of the solvent. In comparison to the PLLA/1,4-dioxane system,² the degree of freezing-point reduction in the UV-curable monomer/1,4-dioxane system is observed to be very high. The higher degree of freezing-point reduction in UV-curable monomer/1,4-dioxane system should increase the degree of supercooling and decrease the channel diameter when compared to the same properties in the polymer/1,4-dioxane systems. However, the experiments showed opposite results: the channel diameter in the UV-curable monomer/1,4-dioxane system was larger than that in the PLLA/1,4-dioxane system. This phenomenon occurs because the degree of supercooling is a function not only of the degree of freezing-point reduction but also of the diffusivity of solute in the solvent as well as surface tension.

Effect of viscosity on channel diameter

In the field of metallurgy, the Mullins-Sekerka theory is often cited to describe the interface instability of crystal growth during unidirectional solidification²⁸: once a perturbation occurs at the interface of the crystal and solution during the solidification as shown in Figure 6, the external thermal flux increases and the crystal growth is enhanced at the

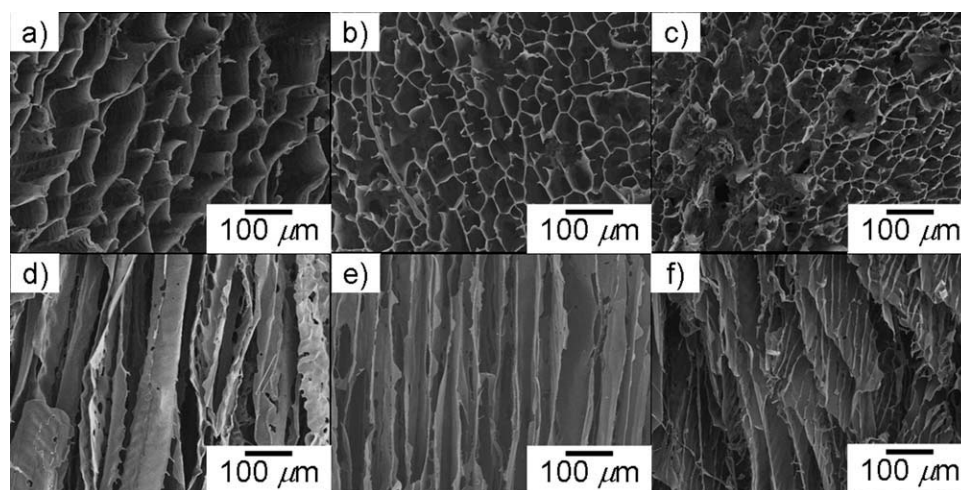


Figure 4 Effect of UV-curable monomer concentration on cell structure. SEM micrographs of porous materials prepared at the immersion rate of 3.5 cm/h: cross section perpendicular to the freezing direction (a–c), cross section parallel to the freezing direction (d–f). Monomer concentrations were 3 wt % (a and d), 5 wt % (b and e), and 10 wt % (c and f).

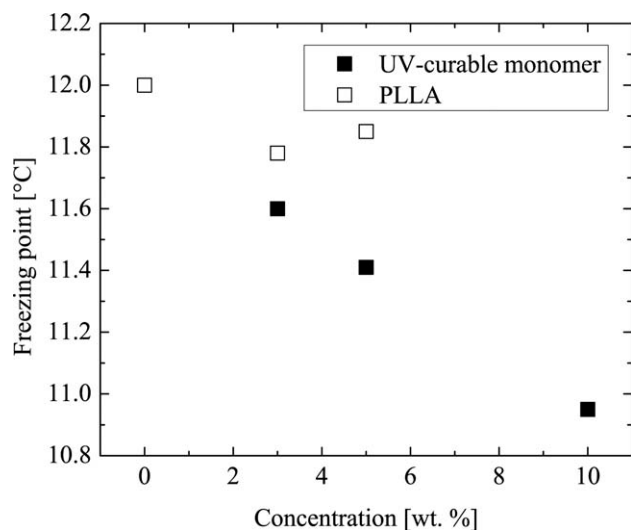


Figure 5 Freezing points of monomer/1,4-dioxane solution (solid square) and PLLA/1,4-dioxane solution (open square).

tips of the interface. On the other hand, at the depressions of the interface, the internal thermal flux increases and the crystal growth is retarded. Thus, only tips of the interface prominently grow in the same direction with the freezing direction. The wavelength of the interface perturbation, λ , is given by³¹:

$$\lambda = 2\pi \left(\frac{D \cdot \sigma}{V \cdot \Delta T \cdot \Delta S_f} \right)^{1/2} \quad (1)$$

where D is the diffusion coefficient, σ is the interface energy, V is the freezing rate, and ΔS_f is the melting entropy of the solvent. ΔT is the difference between the liquid temperature, T , and the freezing temperature, T_f (i.e., $\Delta T = T - T_f$).

On the basis of the theory, we calculated the wavelength and compared it with the experimental results. In this study, D was considered to be the

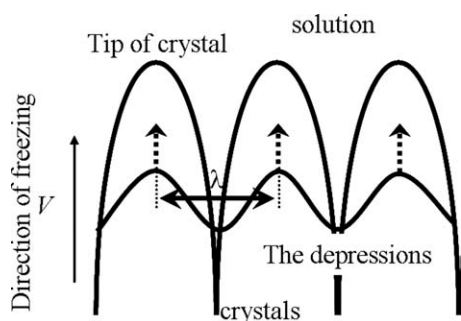


Figure 6 Schematic diagram of crystal growth during unidirectional solidification. (Broken line with arrow shows the direction of solvent crystal growth and indicates that the crystal grows dominantly at the tips of interface.)

diffusion coefficient of monomer in solvent and can be proportional to the solution viscosity.

$$D = K_1 \frac{1}{\eta} \quad (2)$$

Substituting eq. (2) into eq. (1) with some simplified expression gives

$$\lambda = 2\pi \sqrt{\frac{D\sigma}{V\Delta T\Delta S_f}} = K_2 \sqrt{\frac{1}{V\Delta T\eta}} = K_3 \sqrt{\frac{1}{V\Delta T}} = K_4 \sqrt{\frac{1}{V}} \quad (3)$$

For comparing with the experimental results of different freezing rates, all of the parameters, except for V in eq. (3), were considered to be constant and the wavelength λ , therefore, was assumed to be inversely proportional to the square root of the freezing rate, $\lambda = K_4 V^{-1/2}$. All the parameters except for the freezing rate V was lumped into a new constant $K_4 (= 2\pi \sqrt{\frac{D\sigma}{\Delta T\Delta S_f}})$, which could be determined from the slope of Figure 7. In Figure 7, the wavelength λ , determined from SEM micrographs, was plotted against the freezing rate. The monomer concentration was set to 3 wt % in these experiments. Experimental results for this monomer/solvent solution showed a linear relationship between λ and $V^{-1/2}$ and satisfied eq. (3).

Similarly, we plotted the wavelength of the samples and $V^{-1/2}$ for the PLLA/1,4-dioxane system, which is also illustrated in Figure 7 with solid circles. These data indicate that eq. (3) can be applied to both monomer/solvent and polymer/solvent solution systems. Comparing the slopes of two

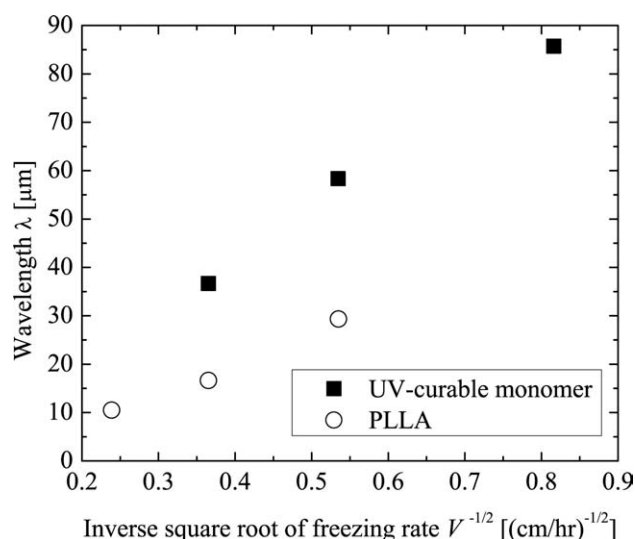


Figure 7 Wavelength versus square root of inverse freezing rate. (All of the UV-curable monomer/solution samples were prepared at 3 wt % monomer concentration.)

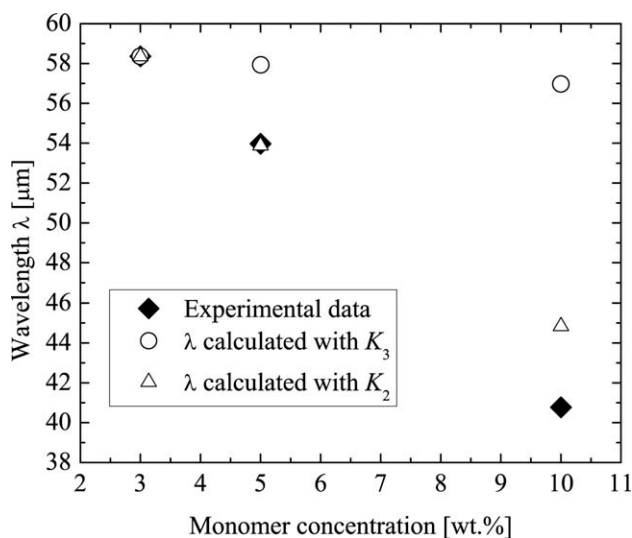


Figure 8 The wavelength of the porous structures (solid squares: experimental data, open circles: λ calculated with K_3 , and open triangles: λ calculated with K_2).

curves in Figure 7, it could be found that although ΔT of the UV-curable monomer/1,4-dioxane system was larger than that of the PLLA/1,4-dioxane system as shown in Figure 5, the K_4 value was larger in the UV-curable monomer/1,4-dioxane system. As K_4 is also a function of $D\sigma/\Delta s_f$ in addition to ΔT , the quantity $D\sigma/\Delta s_f$ of the UV-curable monomer/1,4-dioxane system can be considered larger than that of the PLLA/1,4-dioxane system. It is highly possible that the diffusion coefficient D of the solute is far larger in the monomer/1,4-dioxane system than in the PLLA/1,4-dioxane system due to the difference in molecular weight. The higher diffusivity of the solute could be the reason why the UV-curable monomer/1,4-dioxane systems produce larger cells.

From the data illustrated in Figure 8, in which the monomer concentration was kept at 3 wt % in the solution, we determined three constant coefficients (K_2 , K_3 , and K_4) with the assumptions that the interface energy, σ , between the solid crystal and liquid as well as the entropy variation, Δs_f , were both independent of the monomer concentration and that the diffusivity D (or viscosity η) and freezing-point depression ΔT varied with the monomer concentra-

TABLE I
The Coefficient Parameters Estimated from the Sample Prepared from 3 wt % Solution

Constant parameters	$K_4 \times 10^{-2}$ ($m^{3/2}/s^{1/2}$)	$K_1 \times 10^{-2}$ ($m^{1/2}/K^{1/2}s^{1/2}$)	$K_2 \times 10^{-2}$ ($1/m^{1/2}K^{1/2}$)
Value	181.95	666.05	806.99

tion. At first, K_4 was determined from the slope of Figure 7 to be $181.95 m^{3/2}/s^{1/2}$. K_3 in eq. (3) was calculated by reading ΔT from the freezing-point curve at 3 wt % monomer concentration using Figure 5 and dividing K_4 by the value of $(1/\Delta T)^{1/2}$. In the calculation, the liquid temperature T was regarded as the temperature far from the crystal front and could be approximated by room temperature ($25^\circ C$). Similarly, K_2 was obtained by measuring the viscosity η of the solution at 3 wt % monomer concentration and then dividing K_3 by the value $(1/\eta)^{1/2}$. The resulting parameter values are listed in Table I. Using these parameter values, we estimated the wavelengths of the samples prepared from the solution at three different monomer concentrations: 3, 5, and 10 wt %. The results are shown in Figure 8 and Table II. The solid diamonds represent the experimentally obtained relationship between the wavelength and the monomer concentration. The open circles represent the estimates calculated by eq. (3) with the K_3 . The calculation simulates the case that the monomer concentration changed only ΔT and the effect of monomer concentration on viscosity was negligible. The open triangles represent the estimates calculated by eq. (3) with the K_2 . This calculation simulates the case that the monomer concentration changes both ΔT and viscosity η . In the calculations, we used the viscosity calculated from the kinetic viscosity measured by the Ubbelohde viscometer and the density at $25^\circ C$. The values of the viscosities, kinetic viscosity, and density used for calculation are given in Table II. As shown in Figure 8, the estimates using the K_3 (open circles) are quite different from the experimental data (solid squares), whereas the estimates using the K_2 (open triangles) show good agreement. K_2 was determined by dividing K_3 with viscosity. The results clearly indicate that the viscosity is the key factor in determining the cell

TABLE II
The Experimental Data and the Estimated Wavelength λ

Monomer concentration (wt %)	Kinetic viscosity (mm^2/s)	Density (g/cm^3)	Viscosity (mPa s)	Freezing point T_f ($^\circ C$)	Wavelength λ (μm)
3	1.438	1.021	1.468	11.6	58.36
5	1.633	1.040	1.698	11.41	53.97
10	2.279	1.041	2.372	10.95	40.77

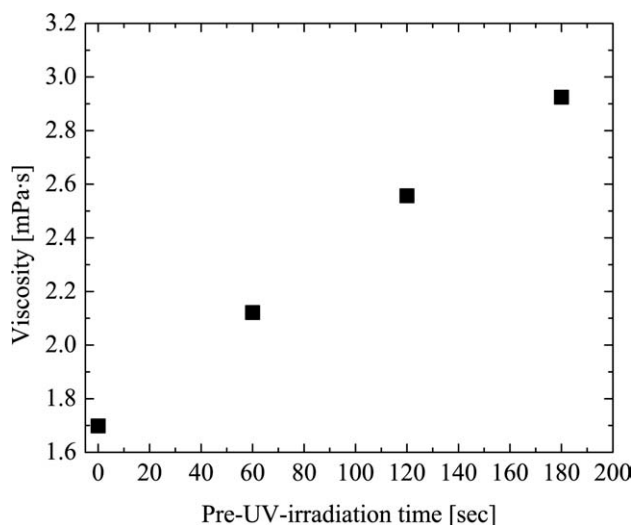


Figure 9 Relationship between pre-UV-irradiation time and the solution viscosity.

structure and can explain why the channel diameter decreases as the monomer concentration increases in the UV-curable monomer/1,4-dioxane system.

Controllability of pore size by pre-UV irradiation

To confirm the effect of solution viscosity and the controllability of the porous structure, the UV-monomer and 1,4-dioxane mixture were treated with UV-light irradiation before unidirectional freezing. The solution viscosity was controlled by changing the irradiation time. Figure 9 shows the relationship between irradiation time and the solution viscosity treated with pre-UV irradiation. As can be seen, the viscosity was increased as the irradiation time was

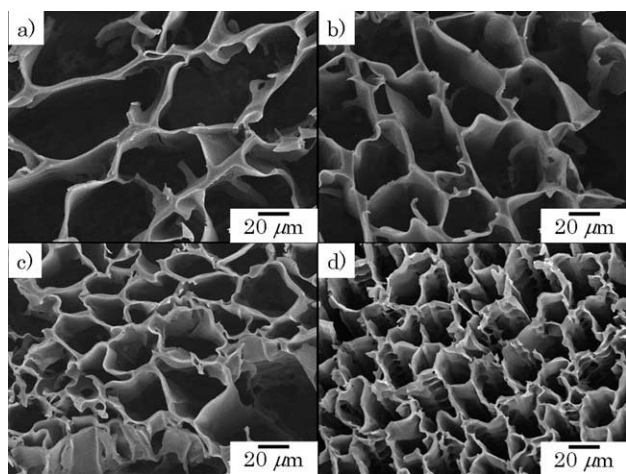


Figure 10 SEM micrographs of the honeycomb monolith structure obtained by the freezing of pre-UV-irradiated solutions of 5 wt %. These are the cross section perpendicular to the freezing direction. Pre-UV-irradiation times are (a) 0 s, (b) 60 s, (c) 120 s, and (d) 180 s, respectively.

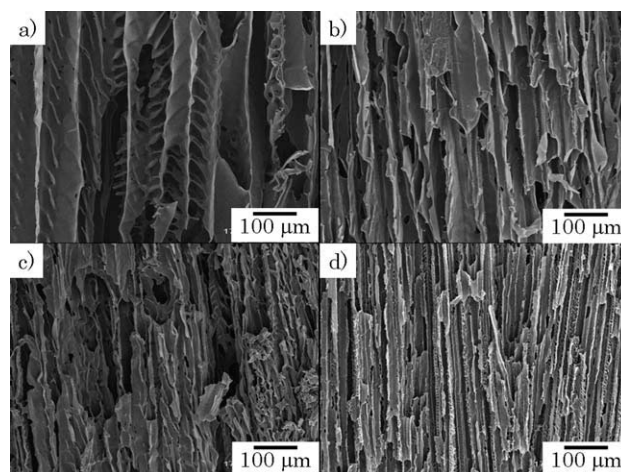


Figure 11 SEM micrographs of the honeycomb monolith structure obtained by the freezing of pre-UV-irradiated solutions of 5 wt %. These are the cross section parallel to the freezing direction. Pre-UV-irradiation times are (a) 0 s, (b) 60 s, (c) 120 s, and (d) 180 s, respectively.

increased. After the pre-UV irradiation, the unidirectional freezing/freeze drying was conducted in the same way as described in the previous section. Figures 10 and 11 show the resulting porous structures. Figure 12 illustrated the relationship between the microchannel diameter and the solution viscosity before unidirectional freezing. The experiments clearly show that the channel size was decreased and the channel wall feature was changed from smooth to dendrite as the solution viscosity was increased. Longer UV-irradiation time increases the solution viscosity, decreases the diffusivity of solute, and consequently, increases the constitutional supercooling.

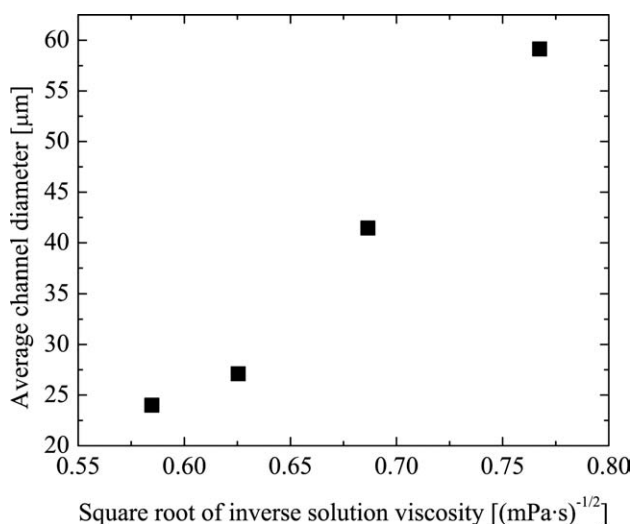


Figure 12 The relationship between the channel diameter and the solution viscosity.

CONCLUSIONS

A micrometer-scale honeycomb monolith porous polymeric structure with aligned channels was successfully prepared by one-directional freezing from UV-curable urethane diacrylate monomer and 1,4-dioxane solutions. The effects of freezing rate and monomer concentration on the porous structure were experimentally investigated. The experiments showed that the faster freezing rate made the wavelength of solvent crystals shorter and the channel diameters the smaller. It was also found that the channel diameter decreased as the monomer concentration increased in solution. The effects of the solution viscosity were examined by changing the UV-irradiation time. It was elucidated that the viscosity of the solution was a hidden factor of controlling the porous structure: The pore size decreased and the microtube wall changed from smooth to dendrite as the solution viscosity increased. UV-curable monomer can keep the solution viscosity lower at freezing stage and provide enough mechanical strength in resultant product by UV polymerization. From the view point of viscosity effect, it can be considered that UV-monomer and 1,4-dioxane system can increase the controllability of pore size of honeycomb monolith structure.

References

1. Hua, F. J.; Park, T. G.; Lee, D. S. *Polymer* 2003, 44, 1911.
2. Kim, J. W.; Taki, K.; Nagamine, S.; Ohshima, M. *Chem Eng Sci* 2008, 63, 3858.
3. Kim, J. W.; Taki, K.; Nagamine, S.; Ohshima, M. *Langmuir* 2009, 25, 5304.
4. Ma, P. X.; Zhang, R. Y. *J Biomed Mater Res* 2001, 56, 469.
5. Schoof, H.; Apel, J.; Heschel, I.; Rau, G. *J Biomed Mater Res* 2001, 58, 352.
6. Ding, S. Q.; Zeng, Y. P.; Jiang, D. L. *J Am Ceram Soc* 2007, 90, 2276.
7. Koch, D.; Andresen, L.; Schmedders, T.; Grathwohl, G. *J Sol-Gel Sci Technol* 2003, 26, 149.
8. Mukai, S. R.; Nishihara, H.; Shichi, S.; Tamon, H. *Chem Mater* 2004, 16, 4987.
9. Mukai, S. R.; Nishihara, H.; Tamon, H. *Chem Commun* 2004, 7, 874.
10. Nishihara, H.; Mukai, S. R.; Tamon, H. *Carbon* 2004, 42, 899.
11. Deville, S.; Saiz, E.; Nalla, R. K.; Tomsia, A. P. *Science* 2006, 311, 515.
12. Deville, S.; Saiz, E.; Tomsia, A. P. *Biomater* 2006, 27, 5480.
13. Araki, K.; Halloran, J. W. *J Am Ceram Soc* 2004, 87, 2014.
14. Fukasawa, T.; Ando, M.; Ohji, T.; Kanzaki, S. *J Am Ceram Soc* 2001, 84, 230.
15. Fukasawa, T.; Deng, Z. Y.; Ando, M.; Ohji, T.; Goto, Y. *J Mater Sci* 2001, 36, 2523.
16. Koh, Y. H.; Song, J. H.; Lee, E. J.; Kim, H. E. *J Am Ceram Soc* 2006, 89, 3089.
17. Moon, J. W.; Hwang, H. J.; Awano, M.; Maeda, K.; Kanzaki, S. *J Ceram Soc Jpn* 2002, 110, 479.
18. Mukai, S. R.; Nishihara, H.; Tamon, H. *Microporous Mesoporous Mater* 2008, 116, 166.
19. Nishihara, H.; Mukai, S. R.; Yamashita, D.; Tamon, H. *Chem Mater* 2005, 17, 683.
20. Fukasawa, T.; Deng, Z. Y.; Ando, M.; Ohji, T.; Kanzaki, S. *J Am Ceram Soc* 2002, 85, 2151.
21. Mukai, S. R.; Nishihara, H.; Yoshida, T.; Taniguchi, K.; Tamon, H. *Carbon* 2005, 43, 1563.
22. Zhang, H. F.; Long, J.; Cooper, A. I. *J Am Chem Soc* 2005, 127, 13482.
23. Zhang, H.; Cooper, A. I. *Adv Mater* 2007, 19, 1529.
24. Kim, J. W.; Tazumi, K.; Okaji, R.; Ohshima, M. *Chem Mater* 2009, 21, 3476.
25. Chino, Y.; Dunand, D. C. *Acta Mater* 2008, 56, 105.
26. Deville, S.; Saiz, E.; Tomsia, A. P. *Acta Mater* 2007, 55, 1965.
27. Waschkes, T.; Oberacker, R.; Hoffmann, M. J. *J Am Ceram Soc* 2009, 92, S79.
28. Mullins, W. W.; Sekerka, R. F. *J Appl Phys* 1964, 35, 8.
29. Jackson, K. A. *Trans Metall Soc AIME* 1966, 26, 1129.
30. Zhang, H. F.; Hussain, I.; Brust, M.; Butler, M. F.; Rannard, S. P.; Cooper, A. I. *Nat Mater* 2005, 4, 787.
31. Kurz, W.; Fisher, D. J., Eds. *Fundamentals of Solidification*, 4th revised ed.; Trans Teck Publications Ltd.: Uetikon-Zurich, Switzerland, 1998, Chapter 3.